

## Electric potential evolution in OH and ECRH plasmas in the T-10 tokamak

A.V. Melnikov, L.G. Eliseev, S.V. Perfilov, K.S. Dyabilin, S.E. Lysenko, V.A. Mavrin, R.V. Shurygin, M.Yu. Isaev, I.A. Krasilnikov, V.I. Zenin, V.F. Andreev, S.A. Grashin, HIBP\* team and T-10 team

*Institute of Tokamak Physics, NRC Kurchatov Institute, Moscow, Russia*

*\*Institute of Plasma Physics, NSC KIPT, Kharkov, Ukraine*

The direct measurement of the electric potential in the core plasma is of primary importance for the understanding of the role of the radial electric field  $E_r$  in confinement regulating mechanisms. The new experimental observations and theoretical description of the formation of  $E_r$  based on NC models in the core and turbulent dynamics in the edge of the T-10 tokamak is the goal of this paper. A Heavy Ion Beam Probe diagnostic was developed for T-10 (circular tokamak,  $B_0=1.5\text{-}2.5$  T,  $R=1.5$  m,  $a=0.3$  m,  $P_{\text{ECRH}}\leq 3.0$  MW) to study the plasma potential with high spatial ( $< 1$  cm) and temporal ( $1 \mu\text{s}$ ) resolution.  $\text{Ti}^+$  ions with energies up to 300 keV were used in T-10 to probe the plasma from the edge to the core [1].

OH and ECRH deuterium plasmas ( $\bar{n}_e = 0.6\text{-}4.7 \times 10^{19} \text{ m}^{-3}$ ,  $T_e < 1 \text{ keV}$ ,  $T_i < 0.6 \text{ keV}$ ) in T-10 are characterized by a negative potential up to  $\varphi(0)=-1300$  V at the core area ( $r=0.1$  m). The density range was significantly enlarged recently towards the lower values and towards the higher values as well, regarding the previous studies. The potential profile is monotonically increasing towards plasma edge for each density in this wide density range. Figure 1 shows the time evolution of the plasma potential and density profiles with density raise due to the gas puff. Figure shows that density rise is accompanied by an increasing negative potential. This is valid for the steady-state phase of the discharge and also for the initial phase of the plasma current and density ramp. Figure 2 (a) shows the time traces of the central chord line averaged density and plasma potential in the mid radius area  $\varphi(0.17 \text{ m})$ . One may see the striking similarity of the density and inversed potential in the Ohmic discharges. Figure 2 (b) shows the potential dependence on density in the wide density range. Figure shows that the density rise is accompanied by an increase in the absolute value of the electric potential. However, if the density approaches certain value  $\bar{n}_e=2.5\text{-}3.5 \times 10^{19} \text{ m}^{-3}$ , the growth of potential saturates. It is worthwhile to note that plasma stored energy is still in the range of the linear growth with density, not reaching the saturation. Interestingly, plasma potential in the TJ-II stellarator with similar size and plasma parameters, also saturates with density of about

$\bar{n}_e = 3.5 \times 10^{19} \text{ m}^{-3}$  in the NBI heated regime [2].

On and off-axis second harmonic X-mode ECRH was applied to heat the OH plasma with  $P_{ECRH} < 3 \text{ MW}$ . Powerful ECRH leads to the increase of  $T_e$  up to 3 keV and strong density profile deformation and decrease the central line-averaged density (“pump-out” ) up to  $\Delta n/n < 30\%$ . Contrary to the density dependence, the rise of  $T_e$  due to the increase of the OH or additional ECRH leads to the decrease of the absolute potential value. Figure 3 (a) shows the time traces of the central chord line averaged density and plasma potential in the mid radius area  $\varphi(0.17 \text{ m})$  in the discharge with auxiliary ECRH. One may see the growth (jump) of the local potential due to the on-axis ECRH, and then recovery to the initial value after the ECRH switch-off. The value of the potential growth  $\Delta\varphi$  does depend on  $\bar{n}_e$ , as presented in Figure 3 (b). It tends to be constant up to certain density value  $\bar{n}_e = 2.5 \times 10^{19} \text{ m}^{-3}$  and then decrease in about two times with the density raise up to  $4.7 \times 10^{19} \text{ m}^{-3}$ .

NC modeling was performed with various codes developed for the rippled tokamak T-10, from the simple analytical approach [3], to neoclassical orbit code VENUS+ $\delta f$  [4] and code DKES with the momentum correction [5]. The radial profiles and the main tendencies like potential decay with density raise and potential raise with  $T_e$  increase due to ECRH are explained by NC models [6]. The potential saturation at high densities is under the consideration now.

As it was described, plasma potential decreases by absolute value, when density decreases. It was recently found that at very low density  $\bar{n}_e = 0.4-0.8 \times 10^{19} \text{ m}^{-3}$  edge potential tends to change its sign to positive at  $0.8 < \rho < 1$ . This data are supported by measurements of Langmuir probes at  $0.97 < \rho < 1$ , which are around +100 V. Edge  $E_r$  becomes almost zero, resembling the potential features in TM-4 tokamak [7] and in stellarators [2, 8]. The ECR heating of such plasmas leads to the formation of the positive plasma potential at the edge.

Direct numerical calculation of the turbulent dynamics in the edge plasma were done with 5-field  $\{\varphi, n, p_e, p_i, W\}$  nonlinear two-fluid MHD Braginskij model, including generalized vortex  $W$  [9, 10]. Equation for electric field is following from ion radial force

balance: 
$$\frac{c}{B_0} \frac{d\phi}{dr} = V_\theta - \frac{c}{eZn} \frac{dp_i}{dr}$$

Analysis shows that diamagnetic term is important for low density case, i.e.  $\bar{n}_e < 1.2 \times 10^{19} \text{ m}^{-3}$ . For higher densities plasma potential is mainly determined by poloidal rotation  $V_\theta(r,t)$ . The modeled potential profiles are shown in Fig. 4.

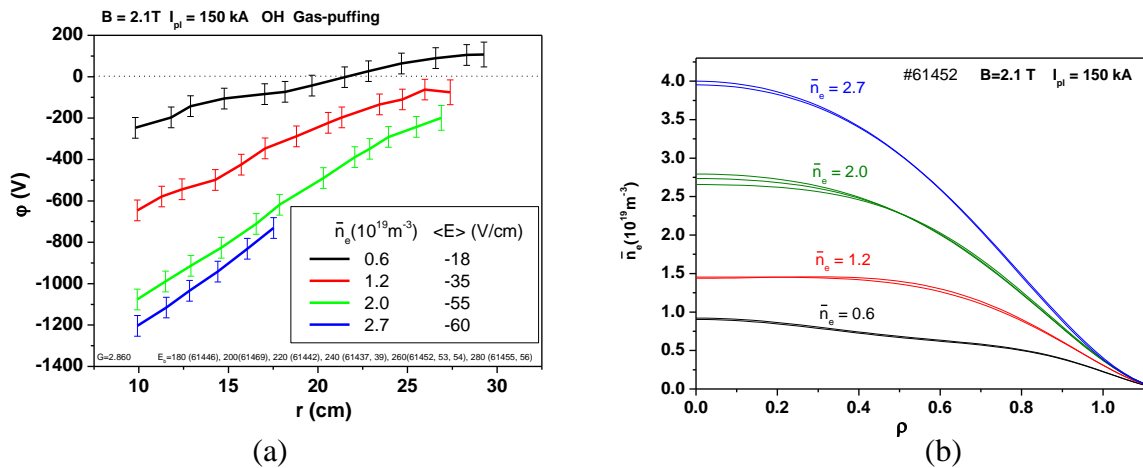


Fig. 1. Plasma potential (a) and density (b) profile evolution due to the gas puff.

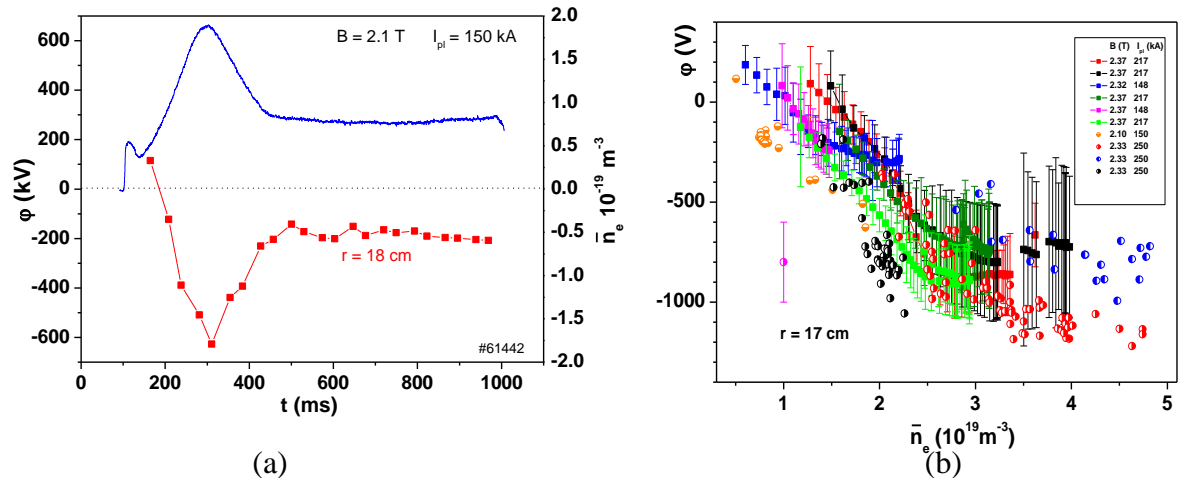


Fig. 2. (a) Plasma potential (red) and density (blue) evolution in the shot with the gas puff. (b) Plasma potential evolution in the wide density range, presented for many shots. Both initial and steady states are presented.

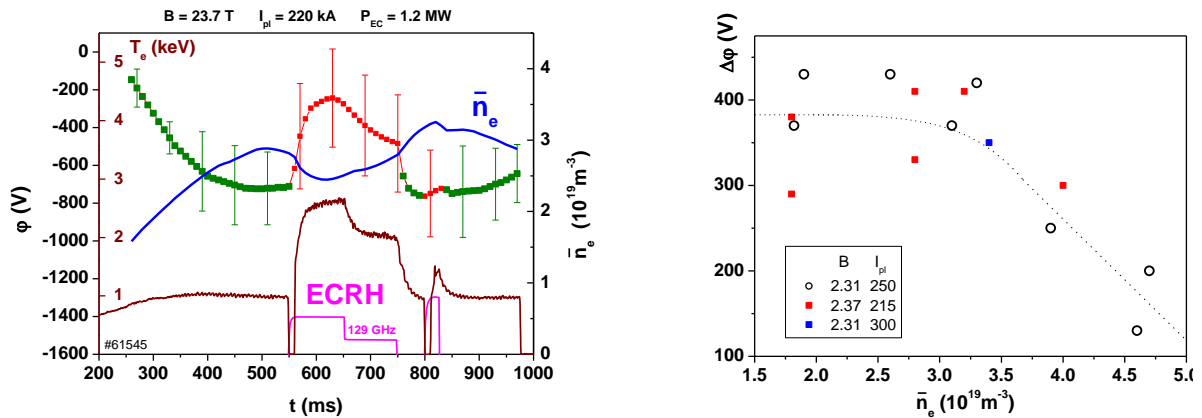


Fig. 3. (a) Plasma potential evolution at  $r = 17$  cm in the shot with auxiliary ECRH, OH-phase (green), ECRH-phase (red). (b) Potential growth due to the ECRH  $\Delta\varphi$  versus plasma density.

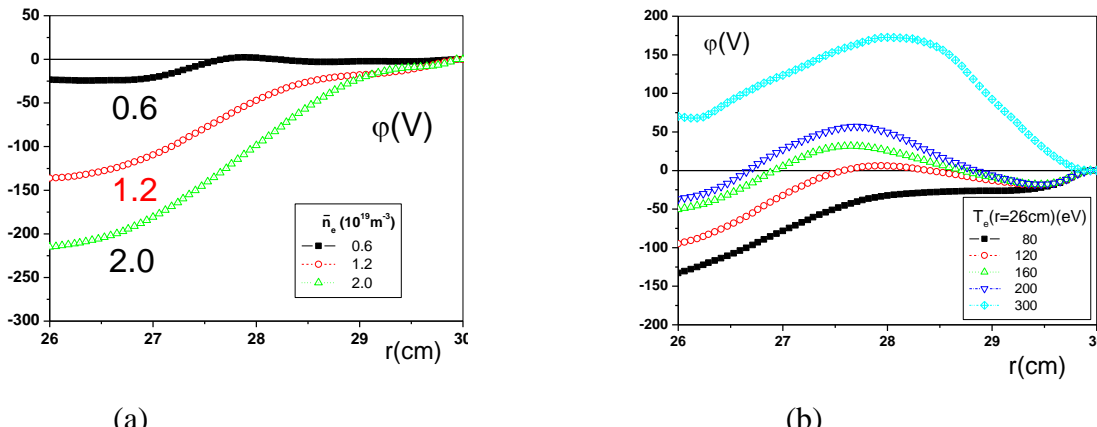


Fig. 4. Modeled edge plasma potential profile evolution. (a) Density raise. Colors and plasma conditions corresponds to Fig. 1. (b)  $T_e$  raise, modeling the ECRH.

Calculation result shows that the model explains the  $E_r$  dynamics due to the influence of the Reynolds stress  $\sim \langle V_{Er} V_{E\theta} \rangle$ , in turn caused by potential phase relations, and Windsor-Stringer force  $\sim \langle (p_e + p_i) \sin\theta \rangle$ .

Note that such behavior can also be explained within NC approach, developed for rippled tokamak, which predicts the change of the potential sign from negative to positive when  $T_e/T_i \gg 1$  in the low collisionality regimes.

In summary, these results indicate the important features of  $\phi$  and  $E_r$  profiles and the non-linear linkage with energy confinement: the linear potential growth with density (confinement time) reaches the saturation at the densities, which are lower than confinement saturation density.

The work is supported by RFBR grants 10-02-01383 and 11-02-00067, Rosatom contract H.4f.45.90.12.1023, Rosnauka grants 16.518.11.7004 and NSh 5044.2012.2.

- [1] A.V. Melnikov et al., *Nuclear Fusion* **51**, 083043 (2011)
- [2] A.V. Melnikov et al., *Fusion Science and Technology* **51**, 31 (2007)
- [3] P.N. Yushmanov, *Nuclear Fusion* **22**, N3, 315 (1982)
- [4] M.Yu. Isaev et al, *Nucl. Fusion* **49**, 075013(2009)
- [5] H. Maaßberg and C.D. Beidler, *Phys.of Plasmas* **17**, 052507(2010)
- [6] M.Yu. Isaev et al., 39-th EPS Conf. on Plasma Physics, (Stockholm, 2012), P2.077
- [7] V.I. Bugarya et al., *Nuclear Fusion* **25**, N12, 1707 (1985)
- [8] A.V. Melnikov et al., *Journal of Fusion Research* **7**, accepted (2012)
- [9] R.V. Shurygin, *Plasma Physics Reports*, **32**, N10, 799 (2006)
- [10] R.V. Shurygin, A.A. Mavrin, *Plasma Physics Reports*, **37**, No 7, 335-350 (2010)